EFFICIENT MODELLING OF SYNCHRONOUS RELUCTANCE MOTOR WITH AXIALLY-LAMINATED ROTOR

X. FENG, K. HAMEYER & R. BELMANS

Katholieke Universiteit Leuven, E. E. Dept., Div. ESAT/ELEN
Kard. Mercierlaan 94, B-3001 Leuven-Heverlee, Belgium

Abstract- An efficient three-dimensional modelling method using an equivalent anisotropic approach for axially-laminated rotors is presented and adopted to analyse the characteristics of synchronous reluctance machines. A three-dimensional realistic model and an equivalent anisotropic model with varying rotor fill-factor have been investigated. The magnetic field and radial flux density distribution, the fundamental and some important harmonics in the air gap are evaluated and compared. Finally, the d- and q-axis inductances and the torque-current angle characteristics of the motor are computed using the equivalent modelling method.

1. INTRODUCTION

The rotor of the synchronous reluctance motor may have various structures in order to increase the ratio of d-axis to q-axis inductance. In the past, some researchers proposed and improved the structures of the anisotropic rotors such as segmented rotors and flux-barrier-rotors [1-11]. From a practical point of view, a promising axially laminated rotor structure is presented. This configuration achieves strong magnetic rotor anisotropy by interleaving the ferro magnetic laminations with non-ferro magnetic spacers. Due to the complex rotor configuration, the finite element analysis proves to be a powerful tool to evaluate the motor behaviour. The finite element analysis requires that each element in the mesh has homogeneous material characteristics. Therefore, both ferro magnetic lamination and non-ferro magnetic spacer in the axially-laminated rotor should be separately subdivided into finite elements during the meshing process of the finite element method. Because non-ferro magnetic spacers and ferro-magnetic laminations are very thin, a large number of elements would be required, otherwise the accuracy and convergence of the solution are worse. In this paper a three-dimensional equivalent anisotropic model for the axially-laminated rotor is presented and adopted to analyse the characteristics of realistic synchronous reluctance motor. Both the realistic and equivalent motor model with anisotropic structure have the same geometry, only the rotor of the realistic model is replaced by a rotor having the same layout but consisting by the anisotropic characteristic material. The realistic three-dimensional model and the equivalent anisotropic model with varying rotor fill-factor, which is defined as the ratio of the non-ferro magnetic insulation thickness to the ferro magnetic thickness in the rotor, have been investigated. Furthermore, the radial flux density distribution, the fundamental and some important harmonics in the air gap are evaluated. Both results calculated from the realistic model and the equivalent model are compared and show good agreement. Using this equivalent modelling method, the torque as a function of the current angle and the rotor fill-factor, the d- and q-axis inductances as the function of the air gap length and rotor fill-factor are computed. Accordingly, the maximum torque can be achieved. The calculated results show that the equivalent modelling is a useful method to handle a strongly anisotropic axially laminated rotor using the finite element method in order to decrease computer memory and computational time by using less finite elements.

2. EQUIVALENT MODELLING IN AXIALLY-LAMINATED ROTOR

A. Equivalent model

In the equivalent anisotropic rotor model, the actual axially-laminated material layout is replaced by anisotropically permeable material. The equivalent permeability in the rotor is (Fig. 1 and Fig. 2):

$$\mu_{xx} = \frac{\mu_I \mu_L (W_L + W_I)}{W_I \mu_L + W_L \mu_I} \tag{1}$$

$$\mu_{yy} = \mu_{zz} = \frac{\mu_L W_L + \mu_I W_I}{W_L + W_I} \tag{2}$$

where μ_L: permeability of the ferro-magnetic laminations
μ_I: permeability of the non-ferro magnetic spacers
W_L: thickness of the lamination
W_I: thickness of the spacer

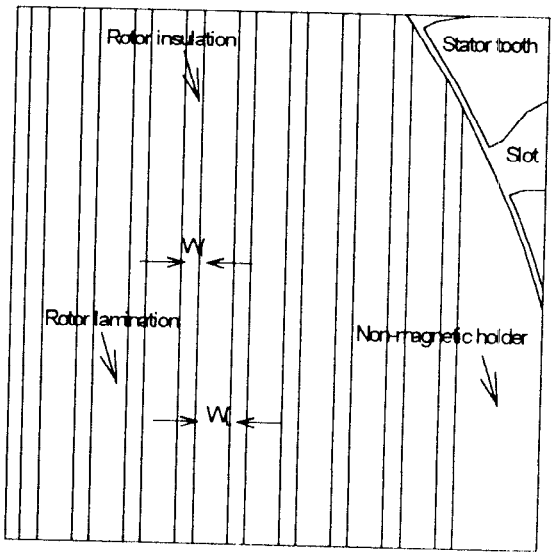

Fig. 1: Zoom of the realistic rotor model

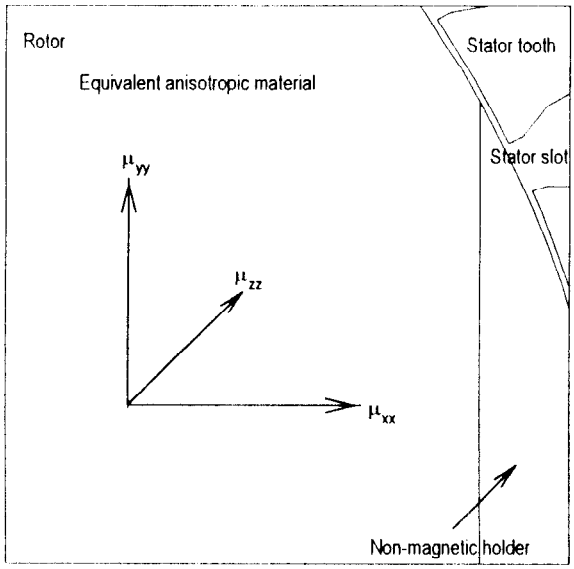

Fig. 2: Zoom of the equivalent rotor

For the equivalent anisotropy model, the relation of the flux density distribution and the field strength is no longer given by a single scalar. A tensor relation is obtained [12]:

$$\vec{B} = \bar{\bar{\mu}}\vec{H} \tag{3}$$

where

$$\vec{B} = \begin{bmatrix} B_x & B_y & B_z \end{bmatrix}^T \tag{4}$$

$$\vec{H} = \begin{bmatrix} H_x & H_y & H_z \end{bmatrix}^T \tag{5}$$

$$\bar{\bar{\mu}} = \begin{bmatrix} \mu_{xx} & \mu_{xy} & \mu_{xz} \\ \mu_{yx} & \mu_{yy} & \mu_{yz} \\ \mu_{zx} & \mu_{zy} & \mu_{zz} \end{bmatrix} \tag{6}$$

with $\bar{\bar{\mu}}$ as permeability tensor. Taking the x-axis as the lamination direction and $\mu_{kj}=\mu_{jk}$ (where j=x, y, z; k=x, y, z; j≠k), the permeability tensor is:

$$\bar{\bar{\mu}} = \begin{bmatrix} \mu_{xx} & 0 & 0 \\ 0 & \mu_{yy} & 0 \\ 0 & 0 & \mu_{zz} \end{bmatrix} \tag{7}$$

A commercial CAD-finite element software package is used to obtain the solution of the equivalent anisotropic model governing the behaviour of the radially laminated synchronous reluctance motor [13].

B. Meshing

The meshing process is the most important step in the finite element analysis of the axially-laminated synchronous reluctance machine. An adaptive meshing results in higher accuracy and a faster rate convergence.

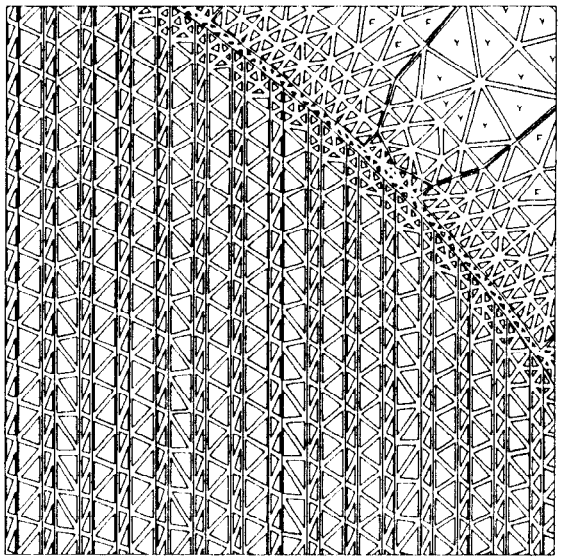

Fig. 3: Zoom of the mesh of the realistic motor model

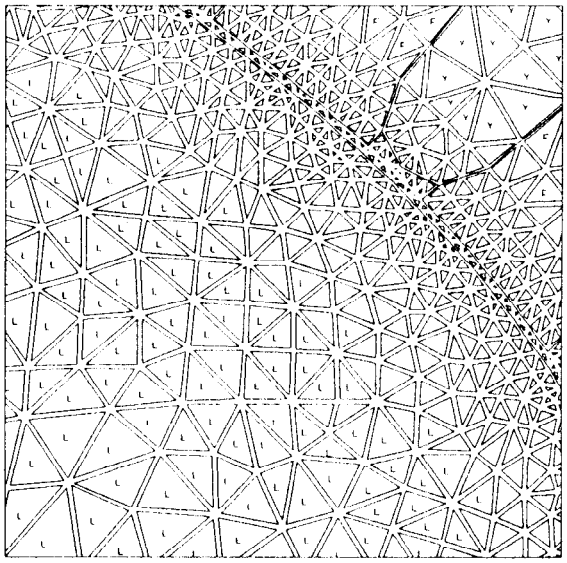

Fig. 4: Zoom of the mesh of the equivalent rotor model

Fig. 3 and Fig. 4 show the zoom of the finite element mesh for the realistic and the equivalent model respectively. The number of nodes and elements in the meshing process of the finite element method used for both models is given in the following table 1.

Table 1: Comparison of realistic and equivalent models

	Number of nodes	Number of elements
Realistic motor	4120	8072
Equivalent model	1953	3828

Clearly, the number of nodes and elements of the equivalent model is less when compared to the realistic model. As the calculation time is approximately proportional to the square of the number of nodes, the advantage is evident, provided the accuracy of the equivalent model is sufficient.

3. d-AXIS AND q-AXIS MAGNETIC FIELD DISTRIBUTIONS AND COMPARISON

The accurate calculation of the magnetic field distribution of the synchronous reluctance motor is important. Many parameters and the performances of the motor can be derived from the magnetic field distributions. Obviously, the magnetic field distribution of the synchronous reluctance motor with axially-laminated rotor depends on the stator exciting current, the stator and rotor constructions such as the air gap length, rotor magnetic lamination thickness, rotor non-magnetic insulation thickness and so on. Here, the synchronous reluctance motor is defined as a magnetostatic problem [12-13].

A. Magnetic field distribution

Defining the rotor salience factor as ratio of the rotor pole-span referred to the rotor pole-pitch, for different rotor fill-factor different rotor salience factor and different air gap length, the d- and q-axis magnetic field distribution of both models is computed (Fig 5-8). The ferro material of the stator and rotor is non-linear, the air gap length is 0.35 mm, the rotor salience factor is 0.67, the fill-factor of the rotor is 0.5.

Fig. 5 and Fig. 6 show the d-axis magnetic field distribution for realistic and equivalent model. Good agreement in both stator field distributions can be found. On the other hand, the d-axis flux in the rotor concentrates on the ferro magnetic laminations in the realistic model (Fig. 5).

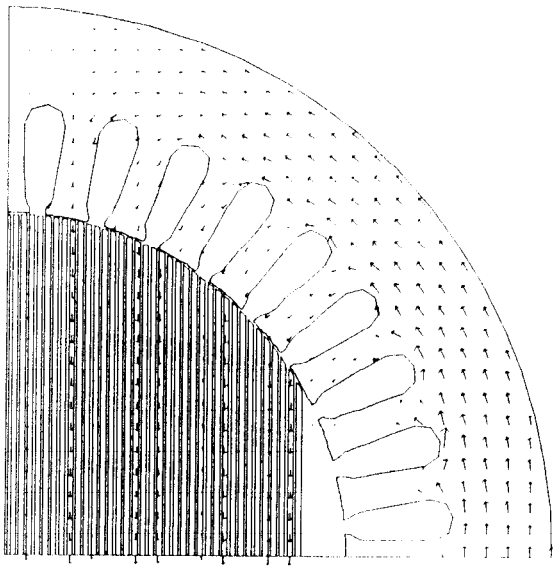

Fig. 5: Field distribution of the realistic model in d-axis

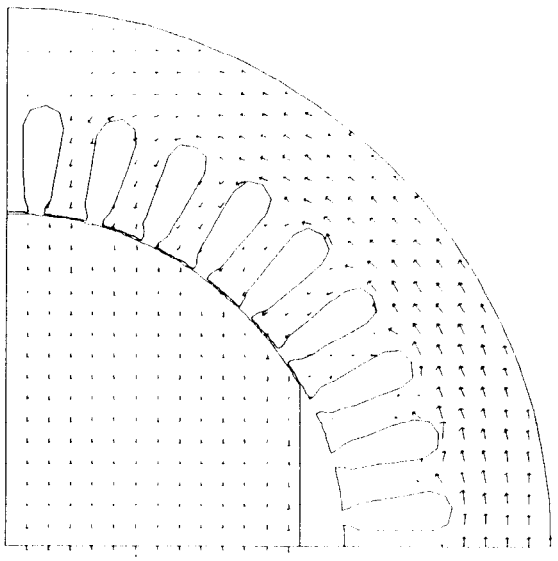

Fig. 6: Field distribution of the equivalent model in d-axis

Fig. 7 and Fig. 8 show the q-axis magnetic field distributions for the realistic and equivalent model. Good agreement can be found for both the stator and the rotor as well. Furthermore, Fig. 7 and Fig. 8 demonstrate that some flux passes through the air gap several times. This is because of the non-ferro magnetic insulations in the q-axis.

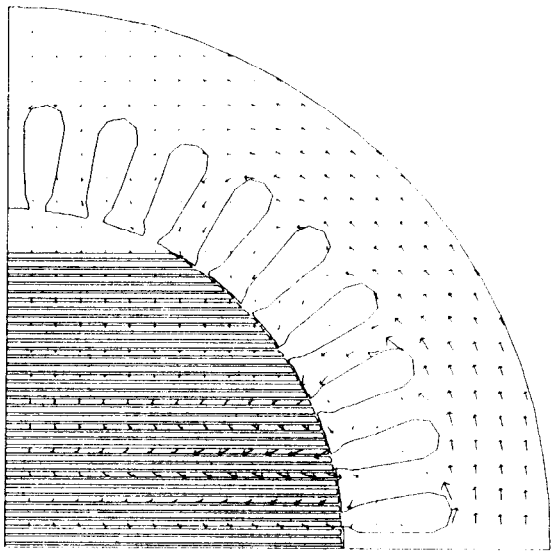

Fig. 7: Field distribution of the realistic model in q-axis

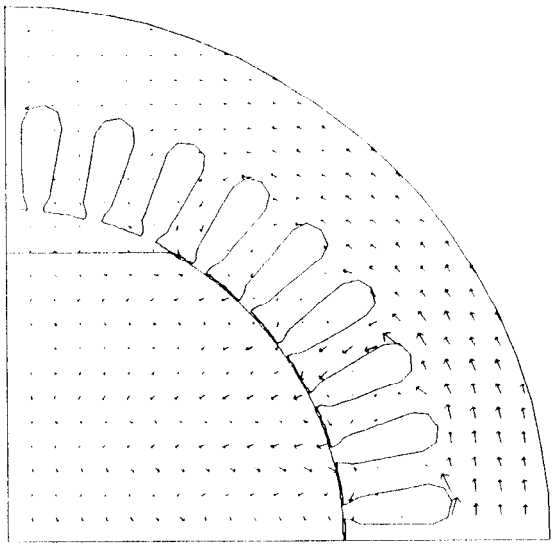

Fig. 8: Field distribution of the equivalent model in q-axis

B. The radial flux density distributions in the air gap

The radial flux density distribution in the air gap along the d- and q-axis is evaluated for both the realistic motor model and the equivalent anisotropic model. One case is shown in Fig. 9 and Fig. 10.

For the d-axis radial flux density distribution in the air gap, the flux density is effected by the stator slots and the non-ferro magnetic rotor insulations. The d-axis radial flux density distribution of the realistic model contains high harmonics caused by the non-ferro magnetic insulations in the rotor. The radial flux density distribution of the equivalent model contains less harmonics when compared to the realistic model (Fig. 9). This means that the equivalent modelling method can't be used to evaluate the harmonic components produced by the non-ferro magnetic insulations of the rotor. The q-axis radial flux passes through the air gap twice under each stator tooth located at the pole span (Fig. 10). This suggests that air gap field in q-axis is rich in stator slotting harmonics.

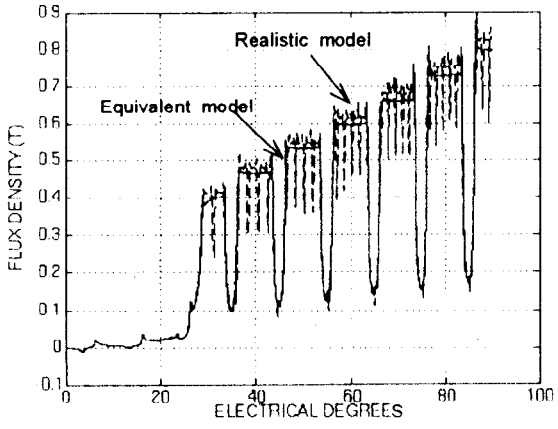

Fig. 9: Radial flux density distribution of the air gap in d-axis

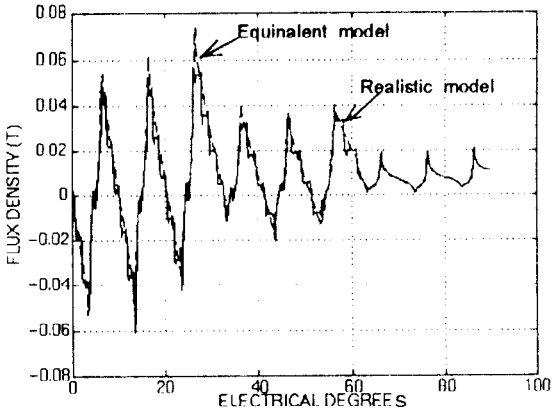

Fig. 10: Radial flux density distribution of the air gap in q-axis

4. HARMONIC ANALYSIS AND COMPARISON

For different rotor fill-factors, the Fast Furrier Transformation (FFT) is applied to study and compare the fundamental and harmonic components of the flux density distribution in the air gap. Normalised spectrums are plotted in Fig. 11 and Fig. 12. They show that the main components of the d- and q-axis flux density distribution are in good agreement as well. For the q-axis flux density distribution there is a leakage field and therefore the corresponding amplitude of the fundamental component is less when compared to the stator slot harmonics.

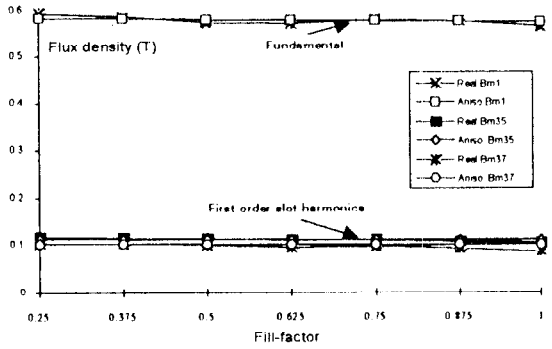

Fig. 11: Main field components in the d-axis field

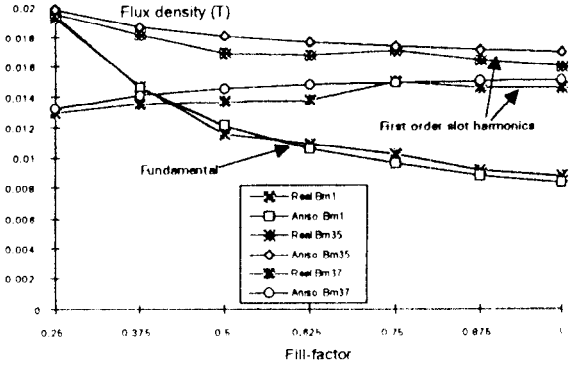

Fig. 12: Main harmonics of the field in q-axis

5. d-AXIS AND q-AXIS INDUCTANCE CALCULATION USING THE EQUIVALENT MODEL

In the design stage, the calculation of the d-axis and q-axis inductance is essential for the assessment of performance for the synchronous motor. It is particularly important when introducing the motor in a drive. It is a simple affair in principle. Indeed, there are several accepted definitions for inductances. As explained by Lowther and Silvester [12], the most fundamental is:

$$L = \frac{2W_{magn}}{I^2} \tag{8}$$

The following formula was derived [14] from the equation above:

$$W_{magn} = \frac{3}{2}\left(\frac{1}{2}L_d I_d^2 + \frac{1}{2}L_q I_q^2\right) \tag{9}$$

Where the stator current space phasor is

$$(I_d + jI_q) = \frac{2}{3}(I_a + I_b e^{j2\pi/3} + I_c e^{j4\pi/3})e^{j\theta} \tag{10}$$

Using the equivalent model and applying a pure d- and q-axis current to the field solution, the corresponding magnetic field energy in d- and q-axis is calculated. Furthermore, L_d' and L_q' as a function of the air gap length and the fill-factor of the rotor are evaluated (Fig. 13 and Fig. 14), supposing that the relative permeability of magnetic material in the model equals to 6000.

The main conclusions to be drawn from Fig. 13 and Fig. 14 are considered to be:

- For the d-axis field of the linear model (Fig. 13), decreasing the air gap length and the fill-factor of the rotor is productive in terms of increasing the d-axis inductance.

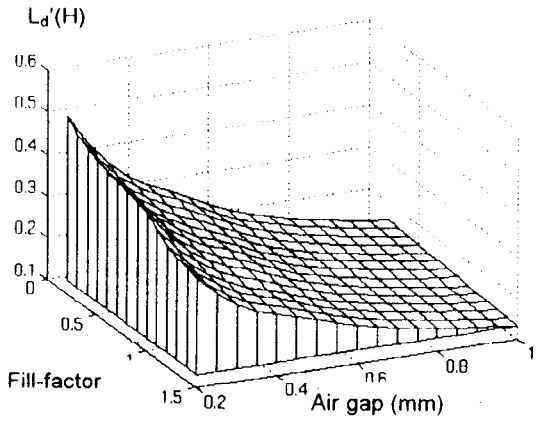

Fig. 13: Inductance of the d-axis as function of the fill-factor and air gap length

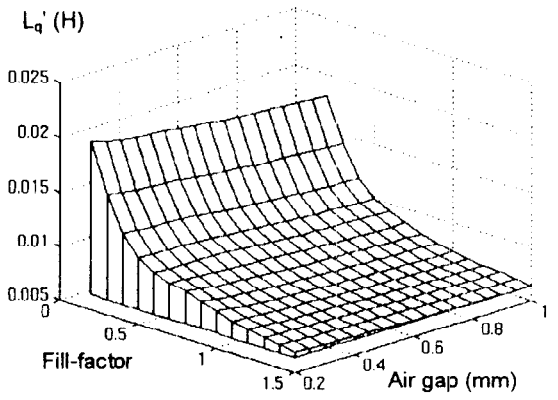

Fig. 14: Inductance of the q-axis as function of the fill-factor and air gap length

- For the q-axis (Fig. 14), the change of the q-axis inductance is very small when the air gap length increases. Especially, it is almost unchanged in the case of rotor fill-factors above 0.4. On the other hand, as the rotor fill-factor increases from 0.2 to 0.4, the decrease of q-axis inductance is larger On the contrary, this change is smaller when increasing the rotor fill factor from 0.4 to 1.5.

6. TORQUE-CURRENT ANGLE CALCULATION USING THE EQUIVALENT MODEL

In order to improve the rotor structure, the torque per Ampere as a function of the load angle and rotor fill-factor has been calculated using the equivalent model for different rotor fill-factors and current angles. The basic principle is based on the change of co-energy of two positions.

$$T = \frac{\Delta W_{co-energy}}{\Delta\theta} \tag{11}$$

Fig. 15 shows that 0.5 of the rotor fill-factor and 45° of the load angle are recommended to achieve the maximum torque per Ampere for this rotor design.

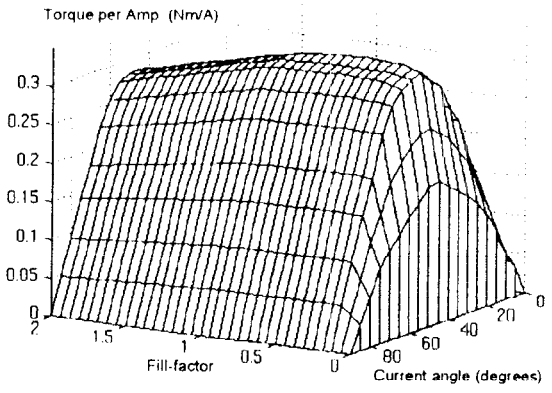

Fig. 15: Torque-current angle characteristic

7. CONCLUSIONS

Equivalent anisotropic modelling of the axially-laminated rotor is an efficient method to evaluate the specific field characteristics of a realistic synchronous reluctance motor with axially-laminated rotor. Using a less fine finite element discretization results in reduced computational costs. Good agreement in d- and q-axis flux density distribution, as well as in the air gap radial flux density distribution is found between the realistic and the equivalent models. A harmonic analysis shows that the stator slot harmonics are not important components for the d-axis and are particularly present in the q-axis air gap flux density distribution. Calculations of the torque-load angle characteristics indicate that 0.5 as the value for the rotor fill-factor is recommended to achieve the maximum torque per Ampere for this rotor design.

ACKNOWLEDGEMENTS

The authors wish to thank the Belgian Nationaal Fonds voor Wetenschappelijk Onderzoek for its financial support for this work and the Belgian Ministry of Scientific Research for granting the project IUAP No. 51 on Magnetic Fields. The authors also acknowledge Katholieke Universiteit Leuven for awarding the scholarship to Mr. Feng.

REFERENCES

[1] P. J. Lawrenson and L. A. Agu, "Theory and performance of polyphase reluctance machines", Proc. IEE, vol. 111, pp. 1435-1445, 1964.

[2] P. J. Lawrenson, "Two speed operation of salient-pole reluctance machines", Proc. IEE, vol. 112, pp. 2311-2316, 1965.

[3] A. J. O. Cruickshank and R. W. Menzies, "Axially laminated anisotropic rotor for reluctance motors", Proc. IEE, vol. 113, pp. 2058-2060, 1966.

[4] P. J. Lawrenson and S. K. Gupta, "Developments in the theory and performance of segmental-rotor reluctance machines", Proc. IEE, vol. 114, pp. 645-653, 1967.

[5] F. W. Htsui, "New type of reluctance motor", Proc. IEE, vol. 117, pp. 545-551, 1970.

[6] J. D. Bak, "Rotor design minimizes magnetic leakage", Design News, No. 5/21, pp. 110-111, 1984.

[7] T. J. Miller, C. Cossar and A. J. Huttan, "Design of a synchronous reluctance motor drive", Proc. of IEEE-IAS Annual Meeting, pp. 122-128, 1989.

[8] T. A. Lipo, "Synchronous reluctance machines-a viable alternative for AC drives?", Electrical Machines and Power System, vol. 19, pp. 659-671, 1991.

[9] I. Boldea and S. A. Nasar, "Emerging electric machines with axially laminated anisotropic rotor", Electrical Machines and Power System, vol. 19, pp. 673-703, 1991.

[10] I. Boldea, Z. X. Fu and S. A. Nasar, "Performance evaluation of axially-laminated anisotropic (ALA) rotor reluctance synchronous motors", Proc. of IEEE-IAS Annual Meeting, pp. 212-218, 1992.

[11] D. Platt, "Reluctance motor with strong rotor anisotropy", IEEE Trans. on Industry Application, vol. 28, pp. 652-658, 1992.

[12] D. A. Lowther and P. P. Silvester, "Computer-Aided Design in Magnetics", New York: Springer-Verlag, 1986.

[13] "MagNet 5 3D ToolBox Reference Manual", Infolytica Corporation, Revised: Oct. 4, 1994.

[14] X. Feng, K. Hameyer and R. Belmans, "Aspects of the Rotor Design of Axially Laminated Synchronous Reluctance Motors", Proc. of. International Conference on Electrical Machines ICEM-96, Vigo, Spain, Sept. 10-12, 1996.